

Infrared Absorption of Pairs of Coupled Local-Mode Oscillators: H^-H^- , D^-D^- , and H^-D^- Pairs in KCl^\dagger

Milton de Souza and Fritz Lüty

Department of Physics, University of Utah, Salt Lake City, Utah 84112

Instituto de Física e Química de São Carlos, Universidade de São Paulo, Est. São Paulo, Brasil

(Received 7 May 1973)

The prototype for a small-mass local-mode defect, substitutional H^- (or D^-) in alkali halides, was used to produce pairs of coupled local-mode oscillators. Pairing was achieved by a thermal reaction of mobile interstitial H_2 molecules with F -center pairs (M centers) in KCl . By alignment of the M centers with polarized light, prior to this reaction, the hydrogen-ion pairs could be created aligned in a particular $[110]$ direction. The use of H_2 and/or D_2 gas in the hydrogenization process allowed the production of H^-H^- , D^-D^- , and H^-D^- pairs in any proportion. From the six expected fundamental vibrations of the pair, infrared-absorption measurements can detect the three optically active in-phase modes of the equal-mass pairs (H^-H^- and D^-D^-). The observed dichroism of the local-mode absorption in crystals with aligned pairs allows a clear identification of the longitudinally and transversally polarized pair modes. For the mixed pair (H^-D^-), three of the six optically active modes could be detected and identified. A simple model for a pair of localized oscillators is presented, which (after the fit of three coupling parameters between the two hydrogen defects) can quantitatively account for the frequencies and polarization of all observed pair modes. The three coupling parameters can be interpreted to arise predominantly from the electric interaction of the two neighboring vibrating dipoles in their longitudinal and transversal configurations. A quantitative fit to this electric-dipole-coupled oscillator model yields effective charges for the H^- and D^- defect close to $1e$. Peculiarities in the widths of the observed local modes are interpreted as arising from transitions between in-phase and out-of-phase pair modes, produced by the emission (or absorption) of an anharmonically coupled lattice phonon.

I. INTRODUCTION

In any study of point defects in crystals, the question will arise at some stage whether or not *pairing* of point defects in specific configurations is possible and can be detected. After the study of the physical properties of the *isolated* defect, it is often interesting to proceed further by investigating the mutual *interaction effects* between a well-characterized pair of these defects. In alkali-halide crystals, many examples of impurity pairs have been studied with various techniques: Na^+1 and F^{-2} and OH^{-3} pairs were detected by ir spectroscopy, Ag^+ pairs in Raman experiments,⁴ and pairs of interacting O_2^- elastic dipoles with EPR techniques⁵—to mention only a few examples. In all these cases, the pairs were produced by a high doping level of the impurities, making use of the statistical probability for a pair formation.

Much simpler and better defined physical conditions can be expected if pairs of defects can be created in a system with low impurity concentration by some specific and controlled *pairing mechanism*. The best-known example for this is the light-irradiation-induced aggregation of F centers, which allows the controlled production of $\langle 110 \rangle$ neighboring F -center pairs (F_2 or M centers) even when starting out with very diluted F -center systems.⁶ The further possibility to align these F -center pairs by selective optical excitation with po-

larized light⁷ allows the detailed study of the optical anisotropy of these pair centers.

It has been known for a long time that substitutional H^- and D^- impurities (U centers) are formed by hydrogen (or deuterium) diffusion into a crystal containing F centers. More recently this defect has attracted wide interest due to the local-mode absorption from the (small-mass) hydrogen vibration.⁸ Extensive experimental studies have been performed on the threefold-degenerate local-mode absorption band as well as on its characteristic phonon sideband structure. A large number of theoretical treatments used this detailed experimental material for the test of various microscopic shell model and anharmonic coupling calculations.⁹ Due to these extensive treatments, the H^- and D^- defects have become the best understood prototype cases for a local-mode defect with a weak coupling to the lattice phonons. On the basis of this well-established knowledge about the isolated H^- defect, it would be very desirable to study the interaction effect between a pair of coupled H^- local-mode oscillators. In CaF_2 crystals with very high H^- doping, some extra lines in the vibrational spectrum have been attributed to U -center pairs,¹⁰ though this assignment had to be very tentative.

A simple way to produce (and align) H^- pairs in crystals with an initially low U -center concentration was recently reported by us.¹¹ This method makes use of the above-mentioned possibility to

produce and to align F -center pairs (M centers) by optical methods. Since the work of Hirai it is known that M centers disappear spontaneously at room temperature in a crystal which contains interstitial hydrogen molecules.¹² This early observation suggested the following formation mechanism for aligned U centers, which is illustrated in Fig. 1 in its consecutive stages.

(A) One starts with a system of statistically distributed U centers.

(B) uv or x irradiation at room temperature converts the U centers into F centers.

In this process the hydrogen leaves the anion lattice site and recombines quickly with another hydrogen, forming a stable interstitial H_2 molecule. The anion vacancy becomes occupied by the electron from the H^+ , thus forming an F center.

(C) By light irradiation in the F band, the F centers can be aggregated into pairs (M centers).

(D) By polarized light excitation, the M centers can be aligned.

(E) The H_2 interstitial, which is mobile near room temperature (RT), cannot recombine with an isolated F center. It can, however, react with the F -center pair, transforming the aligned M center into an aligned U -center pair.

For the $\langle 110 \rangle$ neighboring H^+ pair formed in this process, the six nondegenerate local modes in

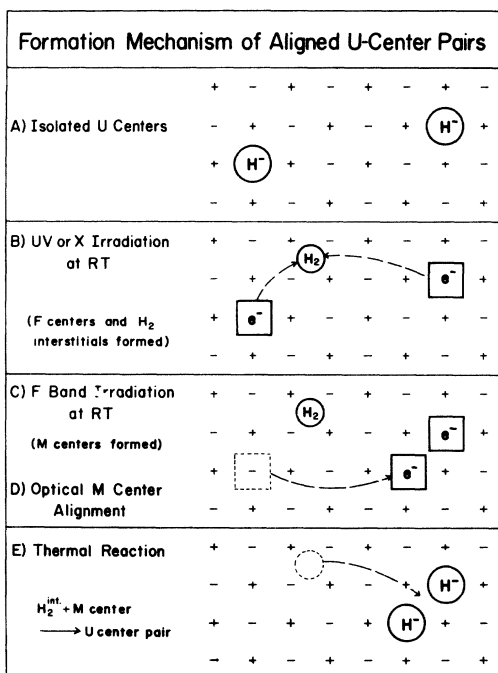


FIG. 1. Schematic illustration of U -center pairing process, producing from a system of statistically distributed isolated H^+ defects aligned pairs of $\langle 110 \rangle$ neighboring U centers.

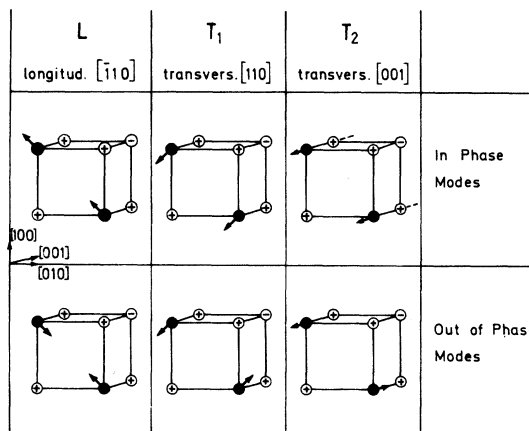


FIG. 2. Illustration of the three in-phase and the three out-of-phase modes and their longitudinal (L) and transversal (T) polarization, for a coupled pair of defect masses on $[1\bar{1}0]$ neighboring anion sites.

C_{2v} symmetry are easily predictable (Fig. 2): They should consist of three *in-phase modes*, which are ir active, and of three *out-of-phase modes*, which are ir inactive for the equal-mass pairs (H^+H^+ and D^-D^-), due to the exact cancellation of the vibrating dipole moments. (The latter modes should, however, be observable with Raman techniques.) For each of the two types of modes there is one polarized parallel to the center axis (longitudinal " L mode"), and two transversal (T_1 and T_2 modes) in the two perpendicular directions, as indicated in Fig. 2. For aligned pairs these modes can be identified by their linear polarization behavior.

In the previously reported initial work,¹¹ the above described pair formation process did indeed produce new local-mode sidebands with a dichroic behavior, which allowed their attribution to the L_1 , T_1 , and T_2 modes of the H^+H^+ pair. In this paper we report more comprehensively about this investigation. The experimental material will be extended to D^-D^- and "mixed" H^+D^- pairs. We will show that the energy position and polarization behavior of all observed H^+H^+ , D^-D^- , and H^+D^- local-mode excitations are in almost perfect agreement with a model for two coupled localized oscillators. The electric-dipole interaction between the two vibrating dipoles supplies the essential part for the coupling. Some peculiarities in the observed width of the pair modes will be discussed and qualitatively interpreted.

II. EXPERIMENTAL PROCEDURES

The KCl crystals grown in the Utah crystal-growth laboratory were first additively colored to the highest possible F -center concentration

($\sim 3 \times 10^{18} \text{ cm}^{-3}$). By heating these crystals at 550°C in H_2 , D_2 , or $(\text{H}_2 + \text{D}_2)$ gas, the F centers were converted into U centers of the desired isotope composition. Cleaved plates with dimensions of about $15 \times 10 \times 1 \text{ mm}$ were x rayed (50 kV, 25 mA) at RT for 2 h on each face, which converts most of the U centers to F centers. A rather homogeneous conversion of the F centers into M centers was obtained by light irradiation at about -5°C into the short-wavelength tail of the F band at about 475 nm. After the optimum M production, the crystals were immediately cooled to liquid-nitrogen temperature for the M -center alignment process. As a first step, the crystal was irradiated with uv light, producing from the remaining U centers a large number of electron traps. The presence of these traps has been shown to be essential for the optical M -center alignment¹³ (which works via temporary M -center ionization¹⁴), and decreases drastically the needed alignment time. The alignment process itself was done by light irradiation with polarized light of 495 nm at liquid-nitrogen temperature. The achieved alignment was monitored by the dichroism of the M band. The system was then heated to RT (or slightly above) for the thermal reaction of the interstitial H_2 molecules with the aligned M centers. This reaction can be monitored directly by observing the decrease of the dichroic M -center absorption. Three to five crystal plates, prepared in this way, were clamped together in a block, inserted into a He cryostat, and were measured at temperatures of 77, 15, and 6°K using a Beckman ir 12 spectrophotometer.

Extremely high concentrations of U centers close to the surface of a crystal could be produced by

heating of a crystal plate at 550°C in an atmosphere of potassium vapor and of H_2 gas (10 atm) for about 1 h. The ir spectra of these crystals displayed local-mode absorptions with the same energy positions as in crystals containing hydrogen pairs produced by M -center reaction.

The U -center pairs, created by either of these two processes, were found to be stable to about 120°C .

III. EXPERIMENTAL RESULTS

A. H^-H^- Pairs

The results on the local-mode absorption of H^-H^- pairs, which have been previously reported,¹¹ are briefly repeated here for completeness. Figure 3 shows the local-mode absorption spectrum of a very high concentrated U -center system in its initial state, and after two subsequent pair-production processes involving M -center reactions. The initial spectrum displays the (off-scale) H^- local-mode absorption at 502 cm^{-1} and its phonon sideband at 565 cm^{-1} , in addition to some very weak bands on both sides of the local-mode line. This initial spectrum changes very little (apart from changes in height) during the first stages (B to D, Fig. 1) of the pair-production process. After the last stage (E), the reaction of the H_2 interstitials with the M centers, however, drastic changes are observed, as seen in Fig. 3. Three bands with approximately equal integrated area develop, with maxima at 535, 512.5, and 463.5 cm^{-1} . The two (unequally strong) bands at 488 and 496 cm^{-1} are found to develop in varying proportions after the pairing process. We ascribe them tentatively to U -center pairs at some-

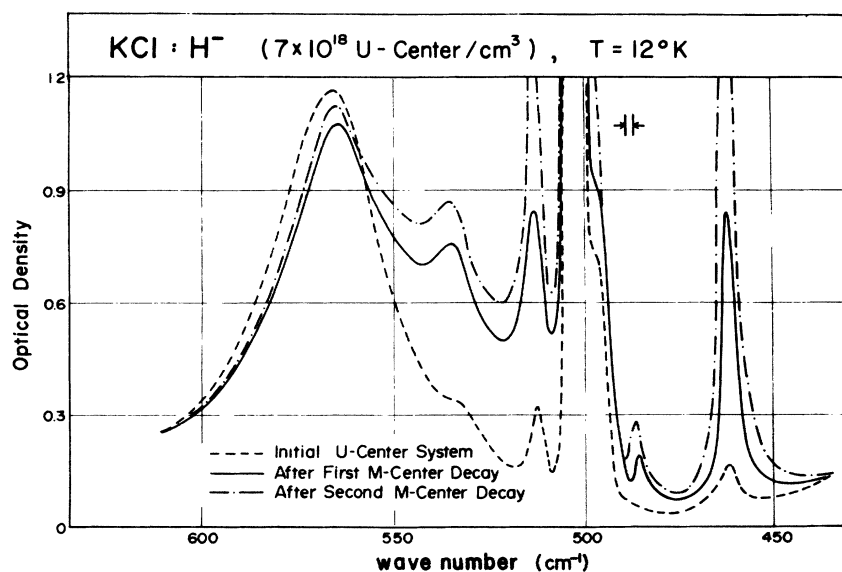


FIG. 3. Infrared absorption spectra of a crystal with high U -center concentration, before and after subsequent treatments, leading to the production of H^-H^- pairs.

what larger distance (e.g., $\langle 200 \rangle$), formed in the same process. We will not discuss them here, as they will be treated in a separate work.

In Figs. 2 and 3 of the previous work¹¹ we have shown the results on dichroic spectra of H^+H^- pairs, which have been produced by H_2 interstitial reaction with aligned M centers. The inserts in these figures explain the geometry of light polarization and aligned pair axes. From these observed behaviors, a definite assignment can be made to the expected local modes in Fig. 2 of this paper: The 463.5-cm^{-1} band is due to the longitudinal (L) mode, the 535-cm^{-1} band is due to the T_1 mode, and the 512.5-cm^{-1} band is due to the T_2 mode. It is very noticeable that the T_1 absorption at 535 cm^{-1} has a much larger width ($\Delta\omega \approx 20\text{ cm}^{-1}$) compared to the width of the L and T_2 absorptions (which become instrument-limited at low temperatures).

B. D^-D^- Pairs

In Fig. 4 (right-hand side), the measured spectrum of the local-mode absorption for a D^- doped crystal after the same pair-production process is plotted. The local-mode absorption of the isolated D^- center is well known to be shifted (compared to the H^- local mode) by a factor 1.394 to smaller energies ($502\text{--}360\text{ cm}^{-1}$). The pair-formation process produces absorptions on both sides of the D^- local-mode line, which look very similar to the H^+H^- pair spectrum (shown for comparison on the left-hand side of Fig. 4). Assigning the observed bands at 331.5 , 375.5 , and 368.0 cm^{-1} (by analogy with the H^+H^- system) to the L_1 , T_1 , and T_2 modes of the D^-D^- pair, respectively, one finds a ratio for the energy positions of the H^+H^- and D^-D^- absorptions, again very close to $\sqrt{2}$ (1.398 for the L band, 1.393 for the T_2 , and 1.424 for the T_1 absorption). Dichroic measurements with aligned D^-D^- pairs (of the type in Figs. 2 and 3 in Ref. 11) clearly confirmed this assignment. In Fig. 6,

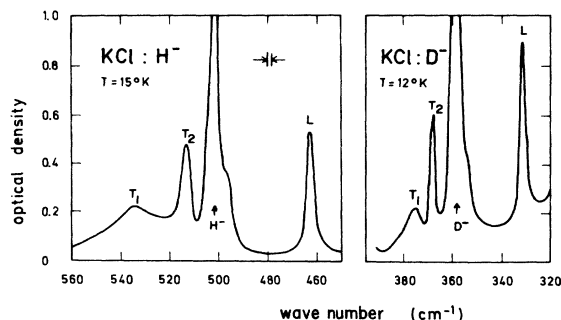


FIG. 4. Comparison of the local-mode spectra of H^+H^- and D^-D^- pairs. (In both cases, the phonon-side-band absorption has been subtracted.)

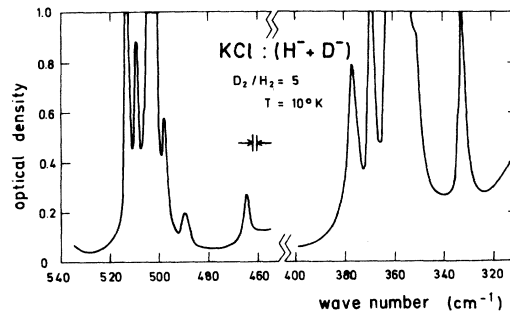


FIG. 5. Local-mode spectra of a U -center system with an isotope ratio $D:H=5$, after production of U -center pairs.

which we shall treat later, such polarized spectra of D^-D^- pairs are included.

Again it is observed that the T_1 absorption is considerably broader than the L and T_2 absorptions; the T_1 bandwidth, however, is smaller for the D^-D^- pair compared to the corresponding H^+H^- absorption. The widths of the local-mode absorptions as a function of temperature were not studied in this work in a systematic way. Some qualitative observations, however, should be mentioned. For both H^+H^- and D^-D^- pairs, the width of the broad T_1 absorption does not change in a noticeable way between 77 and 6°K . The L absorption shows a larger width than the T_2 absorption at 77°K . Upon cooling, however, the width of the L absorption decreases more strongly than the width of the T_2 band, so that at 6°K the L absorption is the narrowest one.

C. H^-D^- Pairs

For the production of mixed pairs, the crystals were hydrogenated in a gas of selected isotope composition. Figure 5 shows the local-mode spectra for a crystal treated with a $D_2/H_2 = 5$ mixture, after the M -center production process. For this case we expect a $25:5:1$ ratio of $D^-D^-:D^-H^-:H^+H^-$ pairs. We indeed observe that the local-mode absorption from D^-D^- pairs is much stronger than that of the H^+H^- pairs. Besides this, however, we observe the appearance of new bands: In the H^- absorption region, two strong lines (at 508.5 and 511.5) appear which are not due to the small H^+H^- concentration. In the region of the (very strong) D^- and D^-D^- absorption, there appears only the indication for one more (unresolved) band at 351 cm^{-1} . Figure 6 shows dichroic spectra for a mixed system after pair production involving $[110]$ aligned M centers. In the H^- absorption region we observe (besides the known dichroism of the H^+H^- L absorption at 463 cm^{-1}) the dichroism of the two new H^-D^- pair absorptions: The

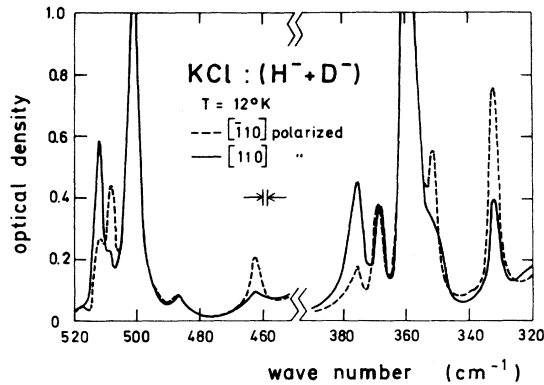


FIG. 6. Local-mode spectra of a U -center system with an isotope ratio of $D:H=5$, after production of $[1\bar{1}0]$ aligned U -center pairs.

band at 508.5 cm^{-1} is polarized parallel to the pair axis (L mode), while the band at 511.5 cm^{-1} is polarized perpendicular in $[110]$, i. e., is a T_1 mode. In the D^- absorption region we first recognize the polarization of the three D^-D^- pair modes L (331.5 cm^{-1}), T_1 (375.5 cm^{-1}), and T_2 (368 cm^{-1}), which is exactly the same as for the three H^-H^- pair modes in the same geometry in Fig. 2 of Ref. 11. This confirms our earlier assignment of these absorptions. The only new H^-D^- band at 351 cm^{-1} shows a polarization parallel to the pair axis, i. e., it should be an L mode.

In Table I all the experimentally observed local-mode absorptions for H^-H^- , D^-D^- , and H^-D^- pairs and their assignment (from dichroic measurements) to L , T_1 , and T_2 modes are listed, together with calculated values obtained from the model derived in Sec. IV A.

IV. DISCUSSION OF RESULTS

A. Coupled Oscillator Model

To set up a simple model, we consider two point masses m_1 and m_2 , occupying two $\langle 110 \rangle$ neighboring anion places in a cubic lattice. The two masses are

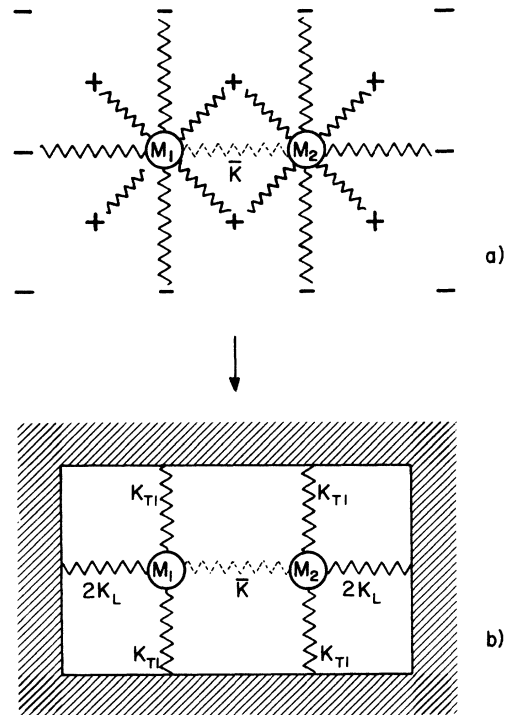


FIG. 7. (a) Illustration of two $\langle 110 \rangle$ neighboring defect masses m_1 and m_2 , coupled to their nearest and next-nearest lattice ion neighbors, and coupled to each other (by the spring K). (b) Replacement of the lattice by a rigid three-dimensional box. The two defect masses are coupled to the box by the (purely longitudinal) effective springs $2K_L$, K_{T1} , and K_{T2} (the latter perpendicular to the plane of the figure), and coupled to each other by spring \bar{K}_α (which has longitudinal and transversal components $\alpha = L, T_1$, and T_2).

coupled to each other by a spring \bar{K} , and are coupled to the other surrounding lattice ions by various other springs [indicated in Fig. 7(a) for nearest and next-nearest neighbors]. Due to the large mass ratio of lattice and hydrogen ion, one can neglect the motion of the lattice ions. We therefore replace the lattice by a three-dimensional fixed box [Fig. 7(b)], to which the masses

TABLE I. Local-mode frequencies (in cm^{-1}) of H^-H^- , D^-D^- , and H^-D^- pairs in KCl as measured by ir absorption and as calculated by the coupled harmonic oscillator model.

U -center pairs in KCl		L modes		T_1 modes		T_2 modes	
		expt.	calc.	expt.	calc.	expt.	calc.
H^-H^-	in-phase	463.5	463.5	535	535	512.5	512.5
	out-of-phase	...	537.7	...	466.6	...	491.3
D^-D^-	in-phase	331.5	331.1	375.5	382.2	368	366.1
	out-of-phase	...	384.1	...	333.4	...	351.0
H^-D^-	in-phase	351.0	350.9	...	352.0	...	357.8
	out-of-phase	508.5	507.4	511.5	506.7	...	502.4

m_1 and m_2 are coupled by effective springs $2K_L$, K_{T_1} , and K_{T_2} (these purely longitudinal effective springs replace all the springs to the lattice ions, but do not include the coupling between m_1 and m_2). The general solution for this system yields

$$\omega_\alpha^2 = \frac{1}{2}(2K_\alpha + \bar{K}_\alpha) \left(\frac{1}{m_1} + \frac{1}{m_2} \right) \pm \left[\frac{1}{4}(2K_\alpha + \bar{K}_\alpha)^2 \left(\frac{1}{m_1} - \frac{1}{m_2} \right)^2 + \frac{\bar{K}_\alpha^2}{m_1 m_2} \right]^{1/2} \quad (1)$$

α stands for L , T_1 , and T_2 , the single longitudinal and the two transversal directions of the vibrations, while the $-$ and $+$ signs yield the in-phase or out-of-phase modes. Whereas each of the effective springs K_α has, by definition, only a longitudinal force constant, the spring \bar{K}_α between m_1 and m_2 has three force-constant components \bar{K}_L , \bar{K}_{T_1} , and \bar{K}_{T_2} .

From this we obtain for the different cases of interest

(i) *Isolated H^- ion* ($m_1 = m_H$; $m_2 \gg m_1$):

$$\omega_\alpha^2(H^-) = (2K_\alpha + \bar{K}_\alpha)/m_H, \quad (2)$$

which, by definition, yields the same value for $\alpha = L, T_1$, or T_2 . (For the isolated D^- ion, the same expression holds with $m_1 = m_D$).

(ii) *H^-H^- pair* ($m_1 = m_2 = m_H$):

$$\omega_\alpha^2(H^-H^-)_{\text{in-phase}} = 2K_\alpha/m_H, \quad (3)$$

$$\omega_\alpha^2(H^-H^-)_{\text{out-of-phase}} = (2K_\alpha + 2\bar{K}_\alpha)/m_H, \quad (4)$$

which will yield different values for the three polarizations $\alpha = L, T_1$, and T_2 . (For the D^-D^- pair the same expression holds with $m_1 = m_2 = m_D$).

(iii) *H^-D^- pair* ($m_1 = m_H$; $m_2 = m_D$): In terms of the eigenfrequencies of the isolated H^- and D^- system [Eq. (2)], Eq. (1) can be written as

$$\omega_\alpha^2(H^-D^-) = \frac{1}{2}[\omega^2(H^-) + \omega^2(D^-)] \pm \left\{ \frac{1}{4}[\omega^2(H^-) - \omega^2(D^-)]^2 + \bar{K}_\alpha^2/m_H m_D \right\}^{1/2}. \quad (5)$$

By comparing one of the observed L, T_1 , and T_2 pair frequencies to the isolated H^- local-mode frequency, we can determine all the K_α and \bar{K}_α parameters. We choose for the fit the three H^-H^- pair modes, and recognize from Eqs. (2) and (3) that

$$[\omega_\alpha(H^-)/\omega_\alpha(H^-H^-)]^2 - 1 = \bar{K}_\alpha/2K_\alpha, \quad (6)$$

which yields

$$\bar{K}_L/2K_L = (502/463.5)^2 - 1 = +0.173, \quad (7)$$

$$\bar{K}_{T_1}/2K_{T_1} = (502/535)^2 - 1 = -0.119 \quad (8)$$

$$\bar{K}_{T_2}/2K_{T_2} = (502/512.5)^2 - 1 = -0.040. \quad (9)$$

With these experimentally determined $\bar{K}_\alpha/2K_\alpha$ val-

ues, all the in-phase and out-of-phase modes of the equal-mass and unequal-mass pair systems are predictable. The result is displayed graphically in Fig. 8: Due to the three different coupling parameters \bar{K}_α , the single local mode of H^- and D^- splits into three optically active in-phase modes L, T_1 , and T_2 (Fig. 8, upper and lower parts). For the mixed pair H^-D^- these three in-phase modes are expected to have a strongly reduced splitting and to be shifted into the D^- local-mode frequency range. Our model predicts [see Eqs. (2)–(4)], that the splitting pattern for the optically inactive out-of-phase modes of H^-H^- and D^-D^- pairs should be the same as for the corresponding in-phase modes, but inverted about the local-mode frequency of the isolated defect (Fig. 8, lower part). For the mixed pair H^-D^- these out-of-phase modes should be shifted into the H^- local-mode region and should have very small splitting.

In Table I we summarize all observed pair absorptions and their experimental assignment (from dichroism) to the L, T_1 , and T_2 modes. These values are compared to the predicted values calculated with our coupled oscillator model by adjustment to the experimental H^-H^- frequencies. As can be seen, the agreement of observed and calculated band positions is very good. All deviations are less than 1%, except for the $D^-D^- T_1$ mode.

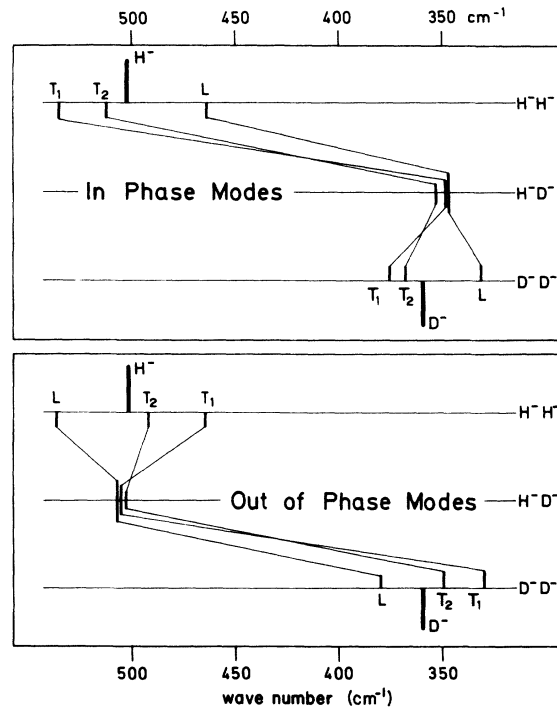


FIG. 8. Energy positions of the longitudinal and transversal in-phase and out-of-phase modes, for H^-H^- , H^-D^- , and D^-D^- pairs.

[This latter may be caused by the relatively large experimental uncertainty in the position of the $\text{H}^-\text{H}^- T_1$ mode, which is very broad and has to be separated from the phonon sideband absorption (Fig. 3).] The observation of the optically inactive out-of-phase modes of the H^-H^- and D^-D^- pairs by Raman experiments would be a very sensitive further test for the validity of the model.

B. Electric-Dipole Coupling

In summary, we have found that the observed pair frequencies can formally be explained by three force-constant parameters \bar{K}_L , \bar{K}_{T_1} , and \bar{K}_{T_2} , which describe the direct coupling between the neighboring H^- or D^- ions during their longitudinal and transversal vibrational motion. What is the physical origin of these (positive or negative) force constants? Compared to the isolated H^- ion, the main difference when adding a second H^- ion is the presence of a vibrating dipole on a neighboring $\langle 110 \rangle$ place. The strongest coupling effect can therefore be anticipated to originate from the electrostatic interaction between the vibrating electric dipoles. The observed *direction* of the energy shift between single ion and pair vibration energy is indeed predicted in the right way by the sign of the dipole-dipole interaction energy. For the in-phase modes (when the vibrating dipoles are oriented parallel), the longitudinal (L) configuration is shifted to lower energies, and the two transversal (T_1 and T_2) configurations shifted to higher energies compared to the energy of a single dipole. (For the out-of-phase modes with antiparallel dipoles it should be just the opposite.) In order to check if the dipole-dipole interaction energy can explain the right *magnitude* of the splitting also, we write the total energy of two harmonic oscillators, coupled by dipole-dipole interaction, as

$$H_\alpha = \frac{1}{2}(m_1\dot{x}_1^2 + m_2\dot{x}_2^2 + m_1\omega_1^2x_1^2 + m_2\omega_2^2x_2^2) + B_\alpha x_1x_2. \quad (10)$$

B_α determines the interaction energy between the dipoles and is given by

$$B_L = \frac{-2e^2}{4\pi\epsilon_0 r^3}, \quad B_{T_1} = B_{T_2} = \frac{+e^2}{4\pi\epsilon_0 r^3}. \quad (11)$$

In terms of the eigenfrequencies $\omega(1)$ and $\omega(2)$ of the isolated oscillators, we obtain from Eq. 10 for the frequencies of the coupled system

$$\omega_\alpha(1, 2) = \frac{1}{2}[\omega^2(1) + \omega^2(2)] \pm \left\{ \frac{1}{2}[\omega^2(1) - \omega^2(2)]^2 + B_\alpha^2/m_1m_2 \right\}^{1/2}, \quad (12)$$

where (1) and (2) can stand for H^- or D^- . Equation (12) is identical to our former Eq. (5) with $B_\alpha = \bar{K}_\alpha$. Formally, we can achieve a fit to the observed pair frequencies by defining for each direction α of the pair vibration a different effective

charge e^* for the H^- ion. We obtain then, e.g., for the case of the longitudinal H^-H^- in-phase vibration

$$e_L^* = \{m_H 2\pi\epsilon_0 (a\sqrt{2})^3 [\omega^2(\text{H}^-) - \omega^2(\text{H}^-\text{H}^-)]\}^{1/2}. \quad (13)$$

We obtain, by fit to the observed H^-H^- pair frequencies

$$e_L^* = 0.648e; \quad e_{T_1}^* = 0.880e; \quad e_{T_2}^* = 0.491e. \quad (14)$$

For a H^- defect with strong ionic character we expect $e^* \approx e$. From the measured integrated local-mode absorption of the H^- defect, a value $e^* = 0.8 \pm 0.1$ has been derived.⁸ We recognize that our values derived from the dipole interaction model lie close to $e^* \approx e$. This clearly shows that the electric interaction energy between the vibrating dipoles has not only the right sign but also the right magnitude to explain the observed splittings. Our "spring-coupled oscillator model" (with the three fitted parameters \bar{K}_α) can be replaced by the "interacting vibrating dipole model" with three fitted e_α^* values; both models are identical and predict the positions of all other pair modes, as listed in Table I.

The assignment of different effective charges e^* to the three coupled vibrations is of course a formal one, and is not justified by any evident physical argument. (More detailed theoretical treatments are in progress to explore possible reasons for differences in e^* .)

In treating the dipole/dipole interaction [Eqs. (11)–(13)] we have completely disregarded the presence of the dielectric host material. It is evident that for large dipole distance ($R \gg a$), the dipole interaction should be screened by the polarization of the host, giving rise to a correction factor (ϵ^{-1}). There is, however, another effect from the presence of the cubic dielectric material: The impurity dipole μ polarizes the surrounding lattice ions in such a way that the effective dipole moment μ_{eff} of the defect becomes enhanced. Calculations of this enhancement¹⁵ due to Lorentz internal field corrections yield $\mu_{\text{eff}} = \frac{1}{3}(\epsilon + 2)\mu$, so that totally a correction factor $[\frac{1}{3}(\epsilon + 2)]^2 (\epsilon^{-1})$ would result from the presence of the cubic dielectric. For our case of interaction of vibrating dipole moments, the high-frequency dielectric constant ($\epsilon \approx 2$) should be appropriate, as the lattice polarization cannot follow the local-mode vibration. With this ϵ value we obtain $[\frac{1}{3}(\epsilon + 2)]^2 \epsilon^{-1} = 0.9$, i.e., a correction factor close to 1. Thus even for large dipole distance R , the influence of the polarizable medium is very small. For our close pair configuration $R = \sqrt{2}a$, the correction from screening and local-field effects can be expected to be even considerably smaller. It therefore seems most appropriate to leave out any dielectric constant effect from Eqs. (11)–(14).¹⁶

While it is conclusive from this analysis that the electric-dipole interaction is the main perturbation, causing the net sign and magnitude of the pair-mode splittings, it is as evident that other anisotropic interaction effects will be present on a minor scale, too, and have to be taken into account in a more refined theoretical treatment. The most important experimental check on possible contributions from interaction effects, other than the dipole-dipole coupling will be the observation of the optical inactive out-of-phase modes for the H^-H^- and D^-D^- pairs by Raman experiments. The coupled dipole model predicts these modes to lie in exact mirror symmetry to the in-phase modes about the isolated U -center local mode. Deviations from this predicted mirror symmetry would thus give direct evidence for the presence and magnitude of other physical interaction effects which are present in the pair configuration.

C. Pair-Mode Bandwidths and Transitions between In-Phase and Out-of-Phase Modes

The bandwidths of the L , T_1 , and T_2 modes show certain peculiarities which have been pointed out before. The most outstanding one is the large width of the T_1 absorption, which is more pronounced for the H^-H^- pair than for the D^-D^- pair. Apparently a very effective decay mechanism must be present for this particular pair mode.

One can ask if, in general, after optical excitation of a particular pair mode, this mode can be transformed (by anharmonic coupling to a lattice phonon) into another pair mode. Such a transition, under emission or absorption of a lattice phonon, could be either to a mode of different polarization (e.g., $L-T$), or to a mode of different phase with the same polarization [e.g., T_1 (in-phase) \rightarrow T_1 (out-of-phase)]. Intuitively, the latter process seems much more likely than the first one: In the latter process, the polarization of the pair vibration is preserved; the weak anharmonic coupling to the lattice has only to change the phase relation between the two linearly vibrating point defects.

In Fig. 9 we consider this latter process somewhat closer. As illustrated in the upper part, a transition from the optically excited in-phase vibration to the out-of-phase mode (of the same polarization) could be achieved by either absorption or emission of a phonon of energy Δ (depending on the sign of the energy difference Δ). The spectral distribution of the density of states $D(\omega)$ of phonons, which couple to the local mode, is approximately given by the phonon sideband of the local-mode absorption.⁸ We assume that this $D(\omega)$ function (which is found to be the same for isolated H^- and D^- defects) describes the coupling of the pair modes to

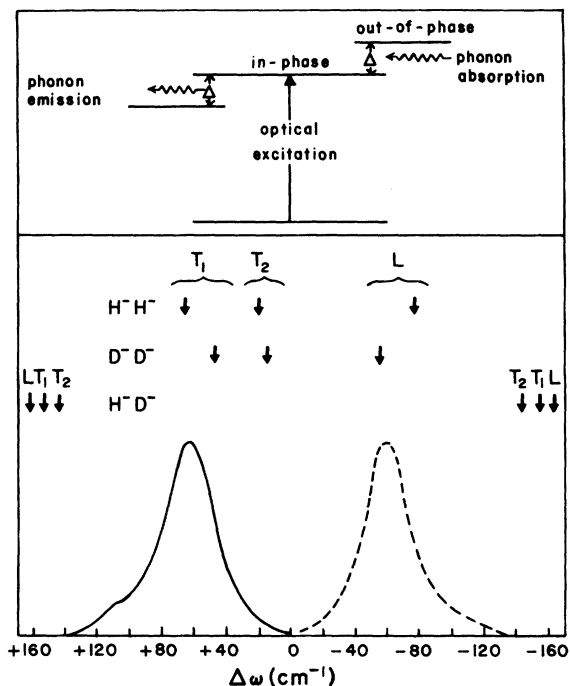


FIG. 9. Upper part: Schematic illustration of transition between in-phase and out-of-phase modes by emission or absorption of a phonon of energy Δ . Lower part: Stokes and anti-Stokes phonon sidebands of U -centers in KCl, taken as the approximate density-of-states distribution $D(\omega)$ for the lattice phonons, which couple to the local mode. The arrows indicate the energy differences Δ between in-phase and out-of-phase vibrations for the various pair modes.

the lattice phonons as well.

In Fig. 9 (lower part), this phonon sideband is displayed as it is measured on the high-energy (Stokes) and low-energy (anti-Stokes) side of the U -center local-mode absorption. In the same figure we indicate by arrows the (positive and negative) energy differences Δ between the in-phase and out-of-phase modes of the H^-H^- , D^-D^- , and H^-D^- pairs. At low temperatures (when only the Stokes phonon sideband is present) the transverse (T_1 and T_2) in-phase modes of the H^-H^- and D^-D^- pairs can decay by phonon emission into the corresponding out-of-phase modes. Following our above arguments, the $D(\omega)$ function gives approximately the probability for such a process. As $\Delta(T_1)_{H^-H^-} = +66 \text{ cm}^{-1}$ nearly coincides with the maximum of $D(\omega)$, this transition will have a very high probability. For the D^-D^- pair this T_1 mode decay will still be strong, but reduced against the H^-H^- case. For both H^-H^- and D^-D^- pairs the decay of the T_2 mode has a small probability. For the L modes no low-temperature decay mechanism is present. This explains qualitatively our observa-

tions: The L absorption has the smallest low-temperature width, followed by the (somewhat wider) T_2 absorptions. The width of the broad T_1 absorption is larger for the H^-H^- pair than for the D^-D^- pair.

At higher temperatures, when phonon absorption processes are also possible, the anti-Stokes side of the $D(\omega)$ curve (right-hand side in Fig. 9) becomes effective. We see that the in-phase L modes of both H^-H^- and D^-D^- should have a high probability to make a transition into the corresponding out-of-phase modes by absorption of a phonon. Again, this is in agreement with the observation: The L absorption (which has the smallest low-temperature width), displays a very strong temperature broadening, and has a large width at 77 °K (see, for example, Fig. 3 in Ref. 11). By comparison, the T_2 mode is only broadened very little in the same temperature range.

For the mixed pairs (H^-D^-) the energy difference Δ between the in-phase and out-of-phase modes is very large ($\sim 150 \text{ cm}^{-1}$) and lies far outside the $D(\omega)$ distribution. A very low decay probability (both by phonon absorption or emission) is therefore expected, which agrees with the observation of very sharp H^-D^- local-mode lines at low and higher temperatures.

It is evident that careful (high-resolution) mea-

surements on the bandwidths of the various pair modes as a function of temperature are needed to test this one-phonon decay model quantitatively. Again the Raman observation of the out-of-phase modes for H^-H^- and D^-D^- pairs will provide the most crucial test: As these modes are expected to have energies (compared to the in-phase modes), which are inverted about the U -center local mode, Fig. 9 would also hold for these Raman-active modes with an exchanged sign of Δ . Now the longitudinal vibration will have a positive Δ close to the maximum probability for phonon emission, while the transversal modes (with $\Delta < 0$) could decay only at higher temperatures by phonon absorption. Thus, a broad L -mode and a narrow T -mode absorption would be expected at low temperatures, with the T_1 mode displaying a very strong temperature broadening. Raman measurements on U -center pairs are under way to test these (and the other) predictions for the model presented here.

ACKNOWLEDGMENTS

Valuable discussions about this work with Dr. H. Bilz, Dr. G. Dick, Dr. J. Page, Dr. G. Ferreira, and Dr. S. Ragusa are gratefully acknowledged.

[†]Work supported by Banco Nacional de Desenvolvimento, Fundo para o Amparo da Pesquisa do Estado de São Paulo, and Conselho Nacional de Pesquisa (Brazil), and NSF Grant No. GH 33704X.

¹T. L. Templeton and B. P. Clayman, *Solid State Commun.* **9**, 697 (1971).

²C. R. Becker and T. P. Martin, *Phys. Rev. B* **5**, 1604 (1972).

³H. U. Beyeler and F. Lüty, *Bull. Am. Phys. Soc.* **18**, 395 (1973).

⁴W. Moeller and R. Kaiser, *Z. Naturforsch. A* **25**, 1024 (1970); and W. Moeller, R. Kaiser, and H. Bilz, *Phys. Lett. A* **32**, 171 (1970).

⁵H. U. Beyeler, R. Baumann, and W. Känzig, *Phys. Kondens. Mater.* **11**, 286 (1970).

⁶For a review of M -center properties, see, for example, W. D. Compton and H. Rabin, *Solid State Phys. Suppl.* **16**, 121 (1964).

⁷C. Z. Van Doorn and Y. Haven, *Phys. Rev.* **100**, 753 (1955).

⁸For a review on U -center properties, see B. Fritz, in *Localized Excitations in Solids*, edited by R. F. Wallis (Plenum, New York, 1968).

⁹H. Bilz, D. Strauch, and B. Fritz, *J. Phys. (Paris) Suppl.* **27**, C2-3 (1966).

¹⁰R. J. Elliot, W. Hayes, G. D. Jones, H. F. MacDonald, and C. T. Senne, *Proc. R. Soc. A* **289**, 1 (1965).

¹¹M. de Souza, A. Gongora, M. Aegerter, and F. Lüty, *Phys.*

Rev. Lett. **25**, 1426 (1970); A. Gongora, Masters thesis (Inst. Politech. Nacional, Mexico, 1970) (unpublished); M. de Souza and F. Lüty, in *Proceedings of the International Color Center Symposium, Reading, 1971*, paper No. 106 (unpublished).

¹²M. Hirai, *J. Phys. Soc. Jap.* **15**, 1308 (1960).

¹³M. Aegerter and F. Lüty, in *Proceedings of the International Color Center Symposium, Reading, 1971*, paper No. 47 (unpublished).

¹⁴I. Schneider, *Phys. Rev. Lett.* **24**, 1296 (1970).

¹⁵G. D. Mahan, *Phys. Rev.* **153**, 983 (1967).

¹⁶In turning the arguments around, one can show that a sizable contribution of ϵ would destroy the good agreement between experimental results and the dipole-interaction model. As the dielectric constant displays a considerable frequency dependence when ω approaches the reststrahl frequency, we have to use a different ϵ value for the region of the H^- vibration (500 cm^{-1}) and D^- vibration (360 cm^{-1}), with $\epsilon(500 \text{ cm}^{-1}) = 1.92$ and $\epsilon(360 \text{ cm}^{-1}) = 1.60$. If ϵ would enter as a simple screening parameter (ϵ^{-1}) into our expressions, the dipole interaction (= splitting energy) of the D^-D^- and H^-H^- pairs should be different by 20% solely owing to this difference in ϵ . The actual measured difference in the splitting energies, however, is fully accounted for by the mass difference $H^- \rightarrow D^-$ and does not allow for any sizable ϵ contribution.